On the effect of the different limiters for the tensor artificial viscosity for the Compatible Lagrangian Hydrodynamics Scheme

Raphaël Loubère
Theoretical Division, T-7, Los Alamos National Laboratory
MS-B284, Los Alamos, NM, 87545, USA
loubere@lanl.gov
LA-UR-05-9301

December 14, 2005

Abstract: In this short note we try to improve the use of a limiter for the tensor artificial viscosity in the context of Lagrangian compatible hydrodynamics scheme for he Euler equations in 2D Cartesian geometry. It has been demonstrated the effectiveness of a limiter on perfectly quadrangular grids aligned with the flow, however if the mesh is not alined with the flow or if it is simply unstructured, then, not only the limiter is not effective anymore but it generates instabilities leading to lack of symmetry. Our goal is to improve such limiters by mean of very simple modifications if possible.

1 Introduction, Context and Presentation

This short note presents the first results of our investigations on the effect of the different limiters in the Tensor Artificial Viscosity (TAV) for compressible hydrodynamics problems. The tensor artificial viscosity has been described in Journal of Computatinal Physics paper JCP, 172 (2001) 739-765 [6] by Campbell and Shashkov. In this paper a subcell-based artificial viscosity is developed, by comparison with a previous work of Caramana and Shashkov, see [8], who developed an edge-based artificial viscosity. Both formulations use a limiter (subcell-based or edge-based) and the improvement of the limiters is the subject of this report.

The context of this study is the Euler equations solved by the compatible Lagrangian scheme with tensor artificial viscosity (see reference [5]) in 2D Cartesian geometry. ALE INC(ubator) [4], a 2D Arbitrary-Larangian-Eulerian code on general polygonal grid for compressible flows, has been used in its Lagrangian regime to carry the experiments. In a previous report [13] we showed that the limiters used in the tensor artificial viscosity, or in the edge viscosity, may generate parasital instabilities when used with unstructured grids. The artificial viscosity without limiter however performs well on almost any grid. Here we shows such cases where the limiter creates instabilities, then we present the reason why limiter are needed. Finaly, we try to modify the limiter in order to be able to deal with unstructured mesh; we only investigate very simple modifications of existing limiters. Several results obtained with these different limiters are presented in this report.

In the rest of this report we present the role of an artificial viscosity module for such a scheme (purpose, effect, limiter form, etc.) in section **2**. Then we present in section **3** the modifications we made to the limiters andin section **4** we present the effect of thses modifications on the well-known Noh test problem in 2D Cartesian geometry on several grids. Finally we conclude this study.

2 Artificial viscosity

The purpose of an artificial viscosity is to allow a numerical Lagrangian scheme to handle steep fronts and shock waves. As a results, using an artificial viscosity leads to shock waves and steep fronts spread over three to five cells. The idea of artificial viscosity dates back to Von-Neumann in his early paper [3]. Since then several attempts have been tried to improve this formulation with more or less success. The very last ones, up to our knowledge, are the edge-based artificial viscosity ([8], [9]) and the tensor artificial viscosity ([6]). These two forms, as well as the original Von-Neumann artificial viscosity, are already implemented in ALE INC.

2.1 Description

Let's briefly describe the role of the artificial viscosity in a Lagrangian numerical scheme for compressible hydrodynamics (we refer the reader to the enlightening paper of Von-Neumann [3]).
Basically, in a Lagrangian scheme there is no dissipative effect, therefore to handle shock wave without spurious oscillations one needs to add an artificial term to the equation which looks like the second spatial derivative of the velocity u: $\partial_{xx}u$. The discretization of such a term spreads the steep front of the shock wave over several cells (usually three to five). When the velocity field is linear or constant this term vanishes. Moreover as the entropy does not increase in expansion fan, there is no need to use artificial viscosity, therefore this term should disappear in this case as well. Finally one needs to detect when this term has to be added or not. Modern form of artificial viscosity only acts when compression occurs; therefore a so-called compression switch is computed in order to turn off the viscosity on region at rest, in uniform motion or in expansion. However it has been pointed out earlier by Caramana *et al.* (see [8]) that such a compression switch is inefficient in the very important case of converging shock wave, as depicted in Fig.1: indeed as a converging shock wave travels through a quadrangular mesh, edges in the radial direction encounter a compression due to the shock wave (edges af, bg, ch, di, ej in Fig.1), the shock wave actually travels across these edges, therefore these edges need the action of the artificial viscosity. On the other hand edges in the angular direction (fg, gh, ij in Fig.1) encounter a compression only due to the cylindrical geometry; no shock wave travels across these edges, hence no artificial viscosity should act on these. In both cases the compression switch detects, as expected, a compression and tells the viscosity to act, however we would like to make the difference between the first case (shock wave compression encountered by edge af) and the second one (cylindrical compression encountered by edge fg); this is the purpose of a limiter.

Paraphrasing Campbell and Shashkov in [6] one can say that Caramana *et al* in [8] specified five properties that an artificial viscosity should posses, these are:

1. Dissipativity: The artificial viscosity must only act to decrease kinetic energy;
2. Galilean invariance: The viscosity should vanish smoothly as the velocity field becomes constant;
3. Self-similar motion invariance: The viscosity should vanish for uniform contraction and rigid-rotation;
4. Wave-front invariance: The viscosity should have no effect along a wave front of constant phase, on a grid aligned with the shock wave;
5. Viscous force continuity: The viscous force should go to zero continuously as compression vanishes and remain zero for expansion.

Caramana *et al.* has been very careful and asked the artificial viscosity to "have no effect along a wave front of constant phase, **on a grid aligned with the shock wave**": he does precise that the grid should be aligned with the shock wave and as we already saw, this property is fulfilled thanks to a limiter, which is therefore not adapted when the grid is not aligned with the shock wave.

Mathematically the tensor artificial viscosity is written as a corner-based entity. However, the first piece of the TAV is the edge-based "q" the form of which was described by Wilkins [2] who attributed it to Kurapatenko [1] (see also [6] for details):

$$q_e = \rho \left\{ c_2 \frac{\gamma+1}{4} |\Delta \mathbf{v}| + \sqrt{c_2^2 \left(\frac{\gamma+1}{4} \right)^2 |\Delta \mathbf{v}|^2 + c_1^2 c_s^2} \right\} |\Delta \mathbf{v}|, \tag{2A}$$

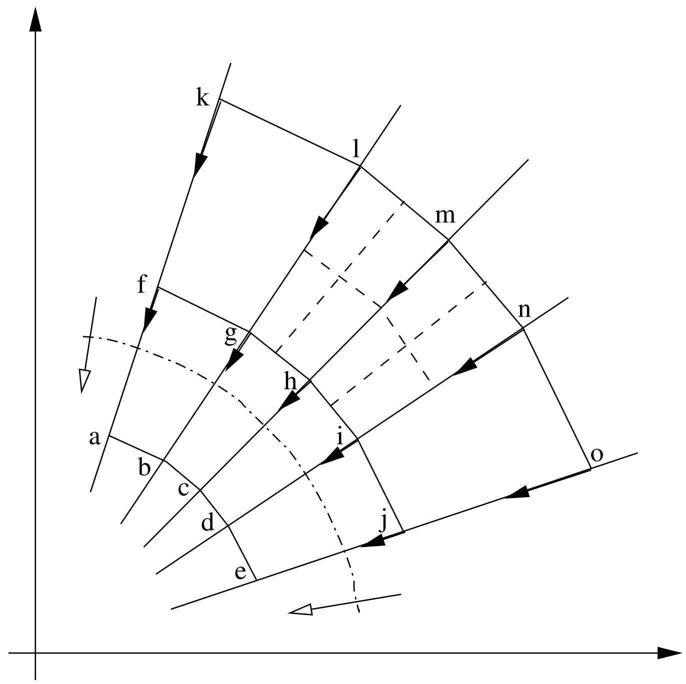

Figure 1: Action of a limiter. A cylindrical convergent shock wave (dashed-dotted line) travels through a quadrangular mesh. Edges af, bg, ch, di, ej encounter compression due to the shock wave traveling across; the artificial viscosity should act. Edges fg, gh, ij encounter compression due to the cylindricity of the problem; artificial viscosity should be turned off on these edges.

where c_1, c_2 are non-dimensional constants usually set to unity, γ is the ratio of specific heats, ρ, c_s the density and sound-speed ahead of the shock and $\Delta\mathbf{v}$ the velocity jump across the shock.
The final form of the TAV subcell force to be added to the scheme reads:

$$\mu_{cn} = (1-\psi_{cn})\ \rho_{cn} \left\{ c_2 \frac{\gamma+1}{4} |\Delta\mathbf{v}_{cn}| + \sqrt{c_2^2 \left(\frac{\gamma+1}{4}\right)^2 |\Delta\mathbf{v}_{cn}|^2 + c_1^2 c_s^2} \right\}\ l_{cn}, \tag{2B}$$

where l_{cn} is a corner length (reflecting the aspect ratio of the corner volume while being relatively insensitive to small changes in the velocity direction see [6] for details) and $|\Delta\mathbf{v}_{cn}|$ is the velocity jump across the corner volume. We do not detail these term as they are "fixed" by the method. On the other hand we focus on the definition of the limiter ψ_{cn}.
The limiter developed for the tensor artificial viscosity is defined as follows: ψ_{cn} is built thanks to the edge limiters ψ_{e_1}, ψ_{e_2} of the two associated edges e_1, e_2 of corner cn

$$\psi_{cn} = \min\left(\psi_{e_1}, \psi_{e_2}\right), \tag{2C}$$
$$\psi_{e_1} = \min\left(\psi_{e_1}^{e_t,e_b}, \psi_{e_1}^{e_l,e_r}\right), \tag{2D}$$

where the top-bottom tb, lr limiters associated with edge e_1 are

$$\psi_{e_1}^{e_l,e_r} = \max\left(0, \min\left(1, R_{e_1}^{e_r}, R_{e_1}^{e_l}, \frac{1}{2}(R_{e_1}^{e_r} + R_{e_1}^{e_l})\right)\right), \tag{2E}$$
$$\psi_{e_1}^{e_t,e_b} = \max\left(0, \min\left(1, R_{e_1}^{e_t}, R_{e_1}^{e_b}, \frac{1}{2}(R_{e_1}^{e_t} + R_{e_1}^{e_b})\right)\right), \tag{2F}$$

and the ratio are defined as

$$R_{e_1}^{e_t} = \frac{(\mathtt{div}\ \vec{u})_{e_t}}{(\mathtt{div}\ \vec{u})_{e_1}}, \qquad R_{e_1}^{e_b} = \frac{(\mathtt{div}\ \vec{u})_{e_b}}{(\mathtt{div}\ \vec{u})_{e_1}}, \tag{2G}$$
$$R_{e_1}^{e_l} = \frac{(\mathtt{div}\ \vec{u})_{e_l}}{(\mathtt{div}\ \vec{u})_{e_1}}, \qquad R_{e_1}^{e_r} = \frac{(\mathtt{div}\ \vec{u})_{e_r}}{(\mathtt{div}\ \vec{u})_{e_1}}, \tag{2H}$$

where $(\mathtt{div}\ \vec{u})_e$ is a discrete approximation of the divergence of the velocity at edge e.
The choice of the left, right, top, bottom edges for a given edge e is made by picking the edge on the left, right making the biggest angle with e and the edges from the two associated cells (said top, bottom) making the biggest angle with edge e; see Fig.2 for an example.
For the structured mesh shown in Fig.2, the choice of left, right, top, bottom edges is obvious, and they are fixed as the simulation goes on (if the mesh is not really distorted during the simulation). On the other hand, if the mesh is unstructured, then the left, right, top, bottom edges are not well-defined at any time and may change in time: this is one of the problem when using a limiter with unstructured mesh.

The final viscosity corner force implemented in ALE INC. involves the limiter and terms of the two adjacent corners in the same cell: cn^-, cn^+ (see Fig.2) and looks like:

$$\vec{f}_{cn} = (1-\psi_{cn^-})\nu_{cn^-}(A_{cn^-}^- + A_{cn^-}^+) + (1-\psi_{cn})\nu_{cn}(A_{cn}^- + A_{cn}^+) + (1-\psi_{cn^+})\nu_{cn^+}(A_{cn^+}^- + A_{cn^+}^+), \tag{2I}$$

where $A_{cn^-}^-$ are terms that involve the first edge of cn^-, $A_{cn^-}^+$ are terms that involve the second edge of cn^-. All the algebra is developed in [6] and we don't repeat here in order not to confuse the reader. The real important point of the previous equation is the fact that the limiter appears in front of each ν_{cn} and $\mu_{cn} = (1-\psi_{cn})\ \nu_{cn}$ (see equation (2B)).

2.2 An illustrative example: limiter works!

A very simple illustrative example is given by the Noh problem in Cartesian 2D geometry on quadrangular mesh. Suppose this problem is solved on a 101×21 and a 101×3 polar grids (101 points in radial direction and $21, 9, 3$ points in angular direction, see Fig.3). In the three cases the angular resolution should not

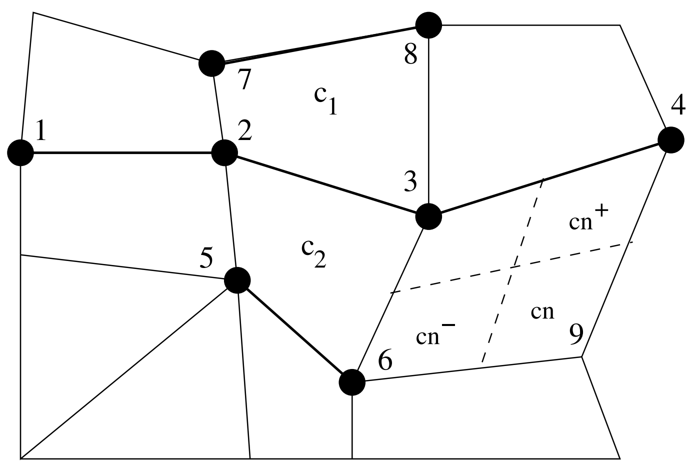

Figure 2: Choice of left, right, top, bottom edges for a given edge e_{23} to be used in the limiter. Left-right edges make the biggest angle with e_{23}, namely e_{12} and e_{34}. Top-bottom edges are edges from cells c_1, c_2 making the biggest angle with edge e_{23}, namely e_{78} and e_{56} — Corner cn has two neighbor corners cn^-, cn^+ in the same cell and two associated edges e_{49} and e_{69}.

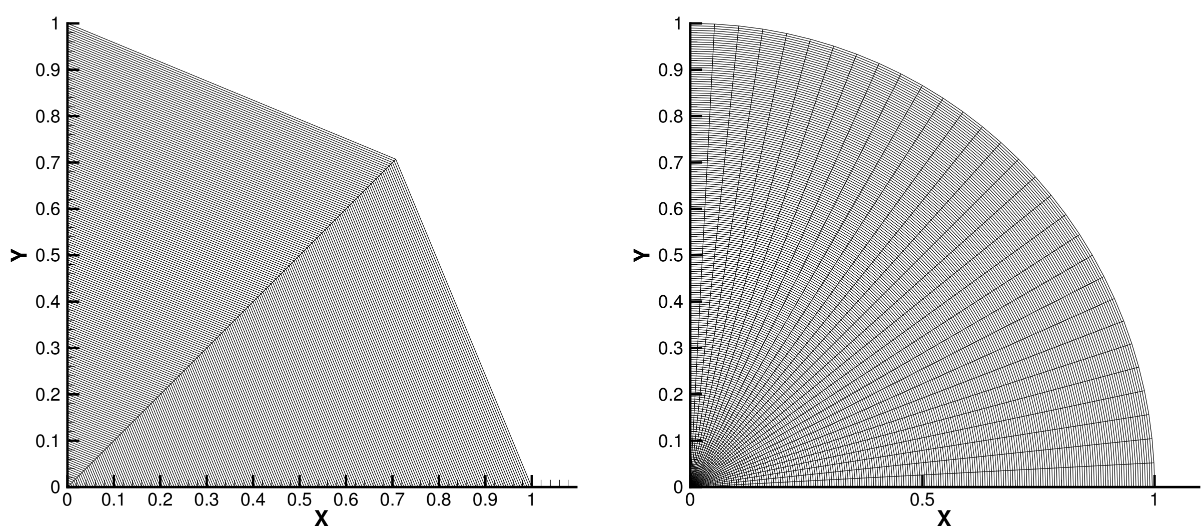

Figure 3: Noh problem in Cartesian geometry for a 101×3 or 101×21 polar mesh — Initial meshes.

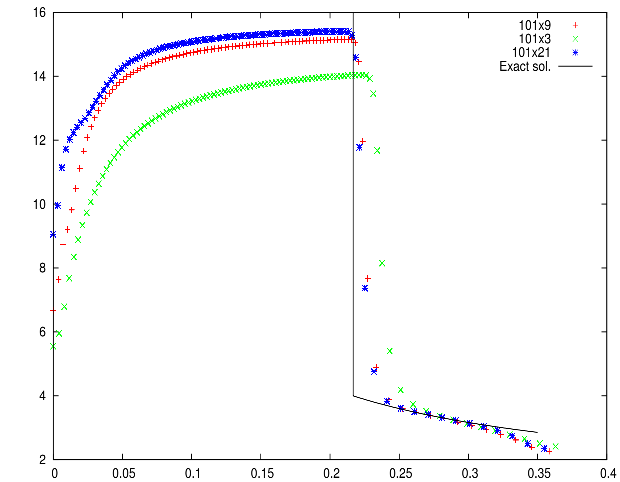

(a)

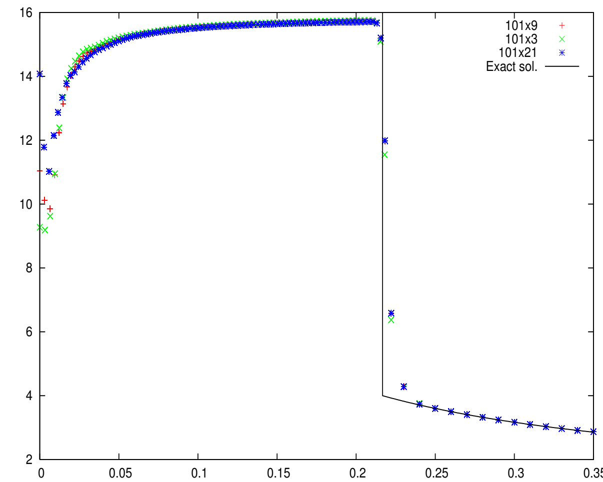

(b)

Figure 4: Noh problem in Cartesian geometry for 101×3, 101×9, 101×21 polar meshes for the tensor artificial viscosity — Density as a function of radius (ALE INC.) at $t = 0.65$ — (a) without limiter the accuracy depends of the angular resolution, (b) with limiter the accuracy is independent of the angular mesh resolution.

matter as far as the symmetry, the accuracy of the shock position and the value of the post-shock plateaus. In Fig.4 is presented the convergence which is obtained with a polar mesh when the number of radio points is fixed 101 but the number of angular cells increases $3, 9, 21$. These plots are the density as a function of the radius for any cell compared to the exact solution (black line) at the final time $t = 0.65$. In theory the angular dimension is ignorable and should not affect the accuracy of the results. However without limiter one gets an improvement of the accuracy, whereas with limiter, the best accuracy is already achieved for the smallest mesh without any improvement as the mesh is refined in the angular direction.

Therefore for this type of mesh the designed limiter works perfectly fine even for a very low angular resolution. Indeed, we are respecting the requirements listed by Caramana in the fourth property the viscosity should fulfill and the limiter works nicely.

2.3 An illustrative example: limiter does not work!

Actually the limiter does not work so well, specifically if the mesh is not nicely aligned with the front wave; the limiter is then not capable to detect any mesh line aligned with the front to turn off the viscosity. Therefore the limiter is like "blind" and it gives wrong information as to turn off or to limit the action of the viscosity. Then on some portions of the mesh the viscosity is limited, on some others it can be simply turned off, and these portions can be different in time due to the dynamics of the problem. Most of the time it leads to severe and dramatic loss of symmetry.

In order to illustrate this behavior let's recompute the Noh problem on a full disk (in order to avoid any boundary effects) with different meshes: a quadrangular polar mesh, well suited for limiter, two triangular meshes obtained by splitting each quadrangle of the previous mesh into two or four triangles (using one or two diagonals) and finally with a real unstructured triangular mesh[1]. In Fig.5 are presented the meshes at $t_{final} = 0.6$ and in Fig.6 the density as a function of radius *versus* the exact solution when the tensor artificial viscosity with limiter is used. The damages caused by the limiter are clearly visible not only on the mesh (the bottom-left mesh presents instability and the top-right mesh has developed a bizarre counter-clockwise spiral motion) but on the loss of 1D cylindrical symmetry as well (bottom-left panels). Only with the quadrangular mesh is the limiter producing good results, but if the mesh is not well aligned with the

[1]The way this mesh is built is of no importance for this illustration therefore we skip this explanation.

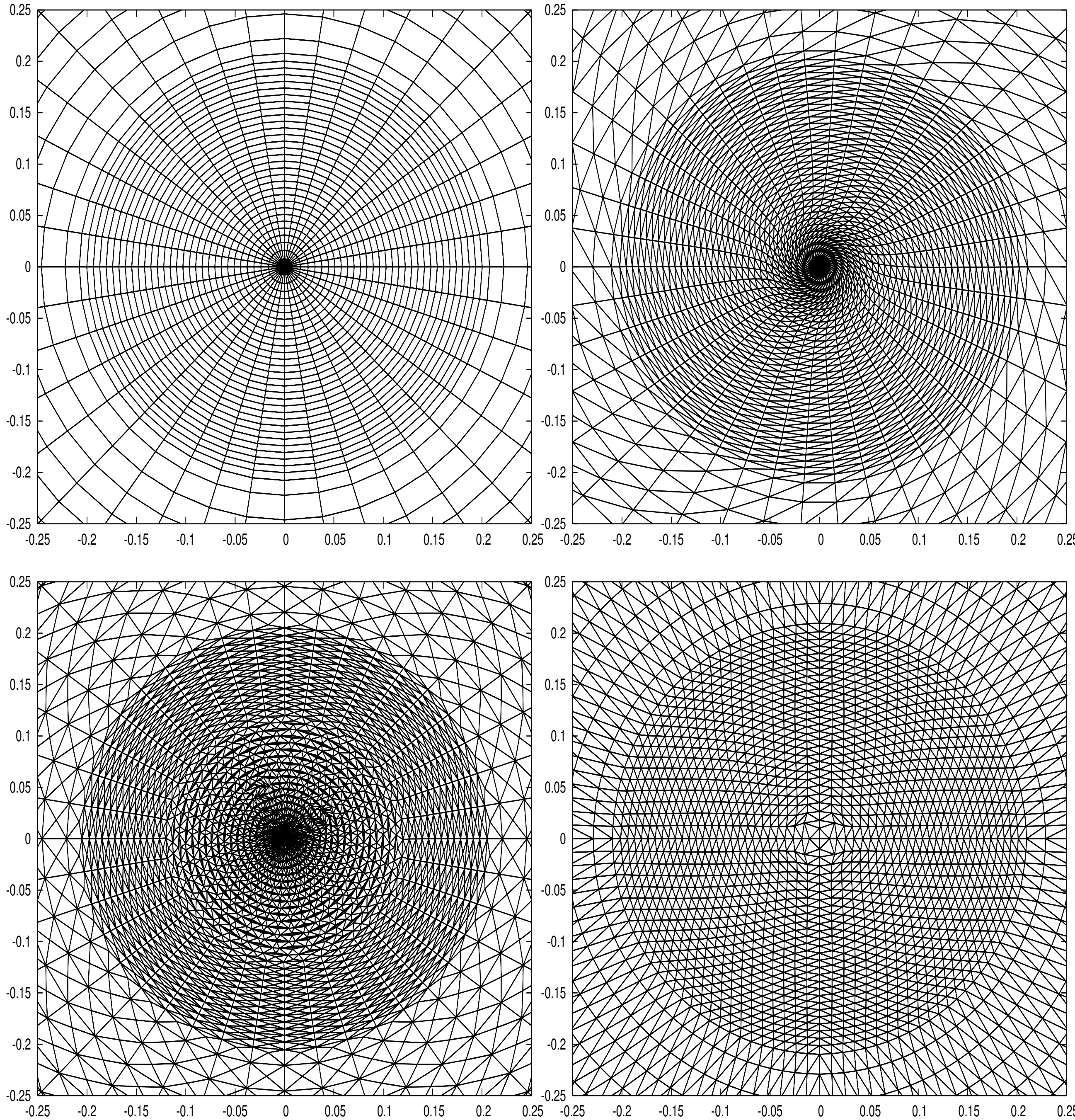

Figure 5: Noh problem at $t_{final} = 0.6$ — Meshes — Tensor viscosity with limiter — Top-left to bottom-right: polar quadrangular, triangular (quadrangle split into two triangles), triangular (into four triangles), unstructured meshes.

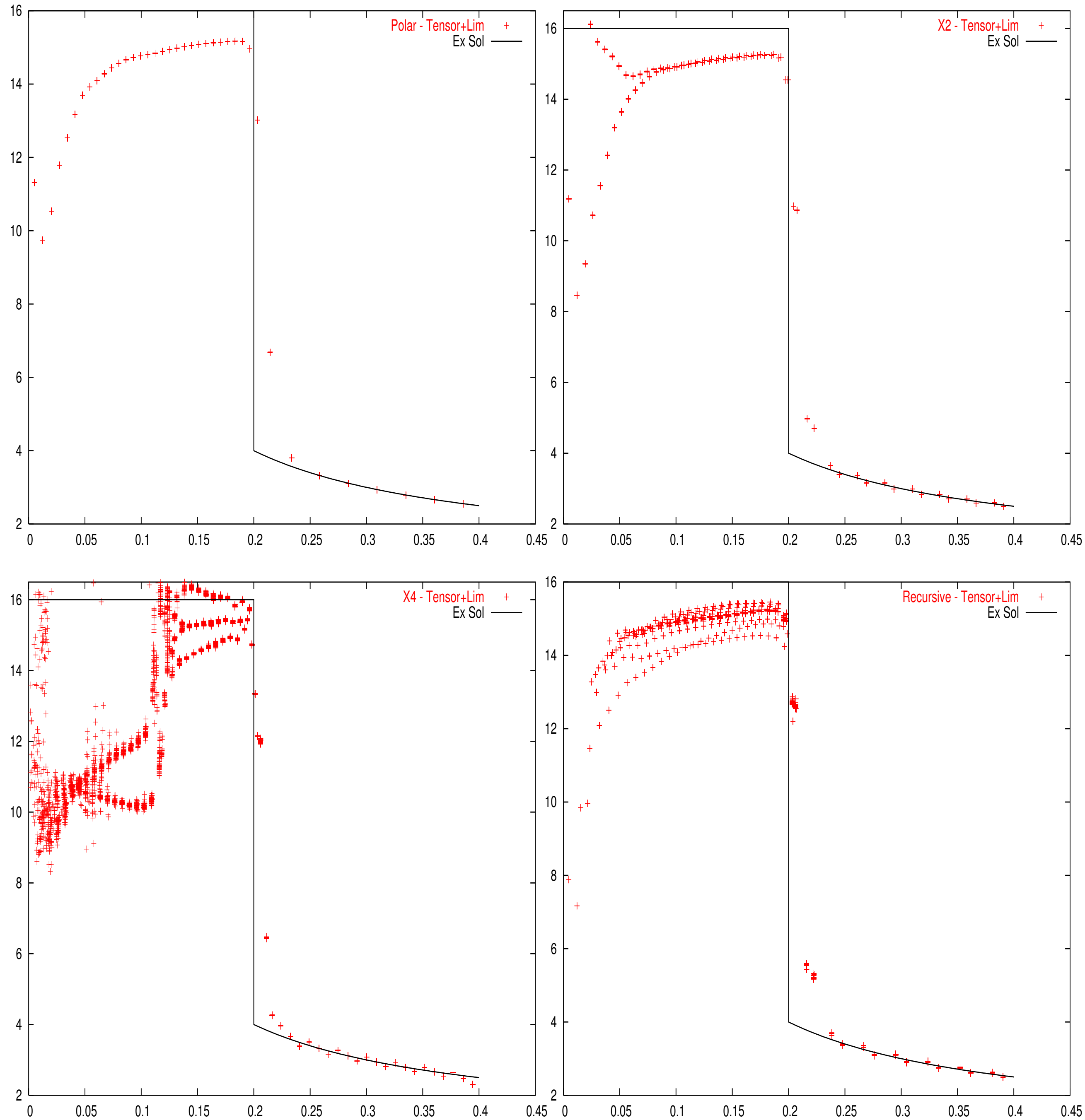

Figure 6: Noh problem at $t_{final} = 0.6$ — Cell density as a function of the cell radius — Tensor viscosity with limiter — Top-left to bottom-right: polar quadrangular, triangular (quadrangle split into two triangles), triangular (into four triangles), unstructured meshes. On the third panel the scale has been reduced to [2; 16] but the oscillation of the density are much bigger.

wave the results are severely damaged.
On the other hand, in Fig.7 and 8, are presented the results obtained when no limiter is used on the same configuration as previously: the symmetry is preserved much more even if the accuracy of the results seems reduced. More specificaly, all points originaly at position (r, θ), with r the radius and θ the angle, seemed to evolve, as expected along the θ-radius line.

Great care has however to be taken, because several triangular meshes may produce symmetrical results even is they look like unstructured triangular mesh. For example the mesh plotted in Fig.9 is one of these ones producing good results when limiter is used, but it is a “fake” good result in the sense that some cancellations occur to annihilate the instabilities which appear and grow otherwise (see [13] for more details).

Then the question of whether or not we should use a limiter in cases where the mesh is not aligned with the flow still remains[2]. In this report we will try to show the behavior of slightly modified limiters on this unique test case.

3 Modified limiters

Limiter can not be modified in any way we choose, several properties have to be fulfilled by the resulting viscosity corner-based forces $\vec{f}_{cn} \equiv \vec{f}_p^z$ (see equ.(2I)):

1. Conservation of momentum:
$$\sum_p \vec{f}_p^z = 0, \tag{3A}$$
the summation of the subcell forces into a given zone z (sum over all points p of zone z) must be zero;
2. Positivity of the heating:
$$-\sum_p \vec{f}_p^z \ . \ \vec{u}_p \geq 0, \tag{3B}$$
the evolution of the cell-centered specific internal energy e_z should always be positive or zero ($\vec{u}_p$ is the velocity of point p). Indeed $e_z^{n+1} = e_z^n + \Delta t \left(-\sum_p \vec{f}_p^z \ . \ \vec{u}_p \right)$ is the discretized PDE associated with the heating.

By construction we already know that without limiter or with the default version of the limiter these properties are fulfilled. However these two properties are affected when changing the form of the limiter, therefore we have to make sure that they are still valid after our modifications.

In the following we will first modified μ_{cn} to make disappear the limiter, that is to say
$$\nu_{cn} = \rho_{cn} \left\{ c_2 \frac{\gamma+1}{4} |\Delta \mathbf{v}_{cn}| + \sqrt{c_2^2 \left(\frac{\gamma+1}{4} \right)^2 |\Delta \mathbf{v}_{cn}|^2 + c_1^2 c_s^2} \right\} \ l_{cn}. \tag{3C}$$
and the force looks like
$$\vec{f}_z^p = \vec{f}_{cn} = \nu_{cn^-}(A^-_{cn^-} + A^+_{cn^-}) + \nu_{cn}(A^-_{cn} + A^+_{cn}) + \nu_{cn^+}(A^-_{cn^+} + A^+_{cn^+}), \tag{3D}$$
and is unlimited in this case. By construction we know that $\vec{f}_{cn}$ fulfills equations (3A-3B). Then we produce new limiters which are not necessarily corner-based ones and test them into ALE INC. However we would like these new limiters to reduce to the old one when the mesh is aligned with the waves, as for the Noh problem with a coarse mesh in the angular direction.

[2] The situation where the user does not know if the mesh is and will remain aligned with the shock waves is highly probable; therefore asking why we want to use a limiter in these cases seem reasonable.

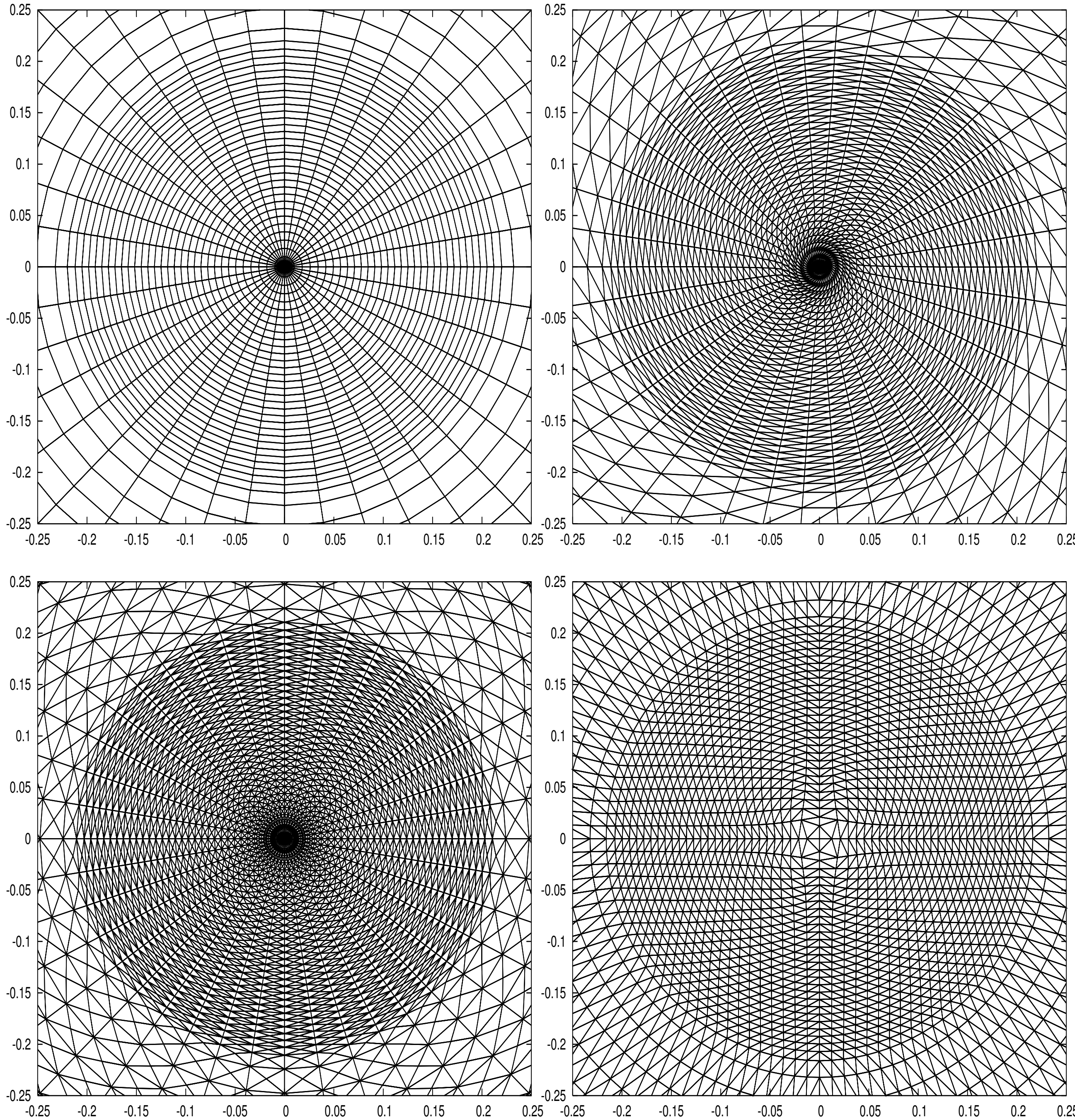

Figure 7: Noh problem at $t_{final} = 0.6$ — Meshes — Tensor viscosity without limiter — Top-left to bottom-right: polar quadrangular, triangular (quadrangle split into two triangles), triangular (into four triangles), unstructured meshes.

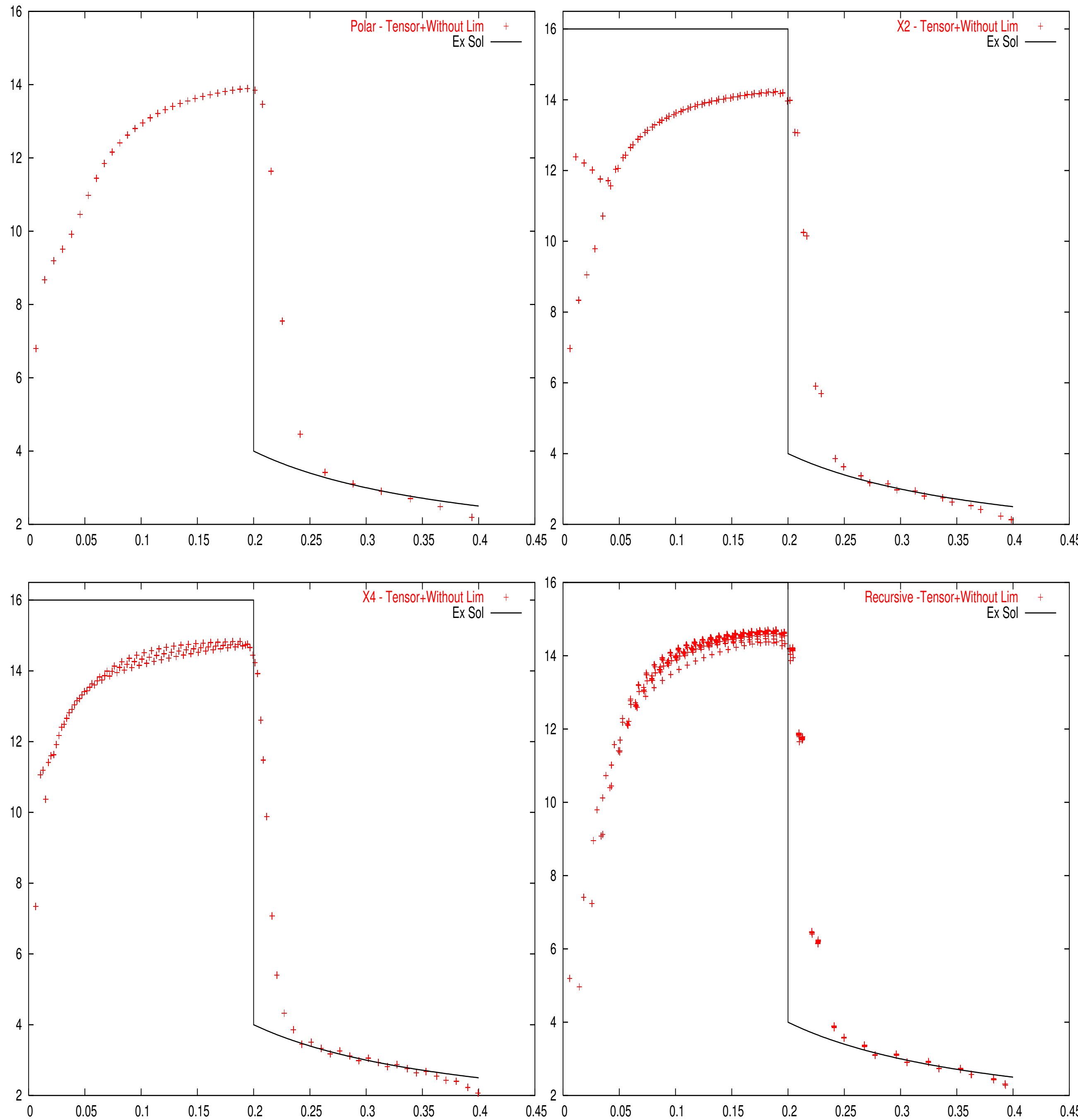

Figure 8: Noh problem at $t_{final} = 0.6$ — Cell density as a function of the cell radius — Tensor viscosity without limiter — Top-left to bottom-right: polar quadrangular, triangular (quadrangle split into two triangles), triangular (into four triangles), unstructured meshes.

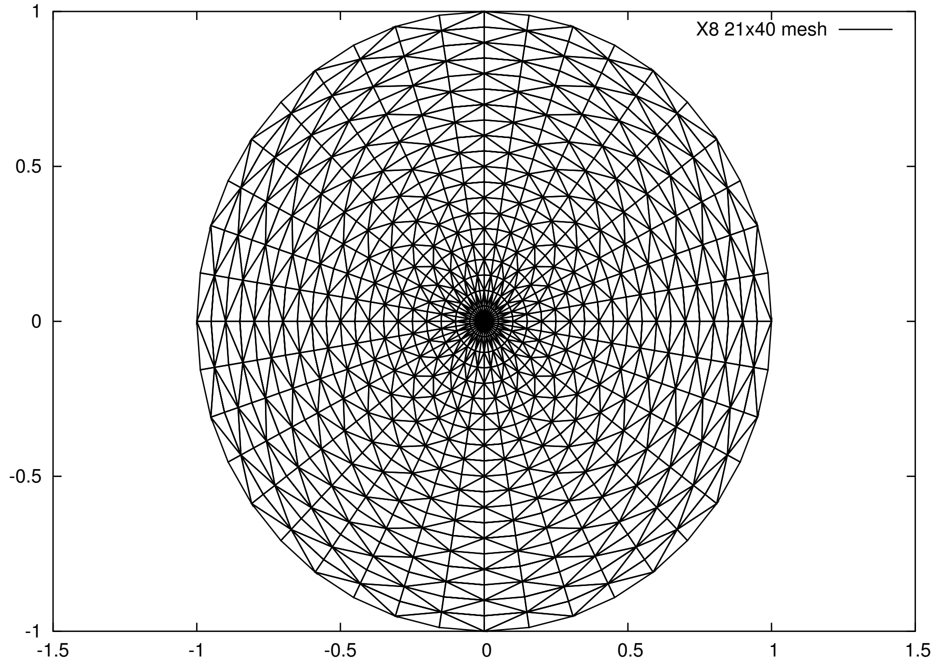

Figure 9: Initial mesh that produces good results on the Noh problem when a limiter is used.

3.1 Cell-based limiter

One modification consists in computing a zone-centered or cell-based limiter ψ_z common for any corner of this zone, then if the limited force is $\vec{F}_p^z = (1-\psi_z)\vec{f}_p^z$, we can show the preservation of the momentum as

$$\sum_p \vec{F}_p^z = \sum_p (1-\psi_z)\vec{f}_p^z = (1-\psi_z)\underbrace{\sum_p \vec{f}_p^z}_{=0} = 0, \tag{3E}$$

where the sum is for all points p of zone z. And the positivity of the heating is obtained thanks to

$$-\sum_p \vec{F}_p^z.\vec{u}_p = -\sum_p (1-\psi_z)\vec{f}_p^z.\vec{u}_p = -(1-\psi_z)\underbrace{\sum_p \vec{f}_p^z.\vec{u}_p}_{\geq 0} \leq 0. \tag{3F}$$

The way ψ_z is computed is simply by:

$$\psi_z = \max_{cn \in z}(\psi_{cn}), \tag{3G}$$

that is to say, the limiter in the zone z is the maximum value of all corner limiters in this given zone. So if at least one corner limiter is equal to 1 then the cell limiter is equal to 1 and the viscosity is turned off in the entire cell therefore for all corner in zone z.

3.2 Edge-based limiter

The limiter developed for the edge viscosity in [8] can be used. This limiter is edge-based and therefore does not need a lot of adaptation to be used in the subcell tensor artificial viscosity.
as already a new We use this limiter into the corner force as the corner force can be split into edge-based

entities (in fact the term $A^-_{cn^-}$ involves the left edge of cn^-); thus each of these terms has an associated edge limiter that we can plug into the force equation:

$$\vec{f}^p_z = \vec{f}_{cn} = \nu_{cn^-}(\mathbf{A}^-_{cn^-} + \mathbf{A}^+_{cn^-}) + \nu_{cn}(\mathbf{A}^-_{cn} + \mathbf{A}^+_{cn}) + \nu_{cn^+}(\mathbf{A}^-_{cn^+} + \mathbf{A}^+_{cn^+}), \tag{3H}$$

where $\mathbf{A}^-_{cn^-} = (1 - \psi_e)A^-_{cn^-}$ and e is the left edge associated with corner cn^-.
The preservation of momentum and the positivity of the heating is obtained trivially as for the edge-based artificial viscosity from [8].

3.3 Corner-based limiter

An other solution is to keep the corner-based form of the limiter but to change the way it is computed. Given the corner-based limiter we assoicated all corners linked together by their node (all corners around one node that basically define the median mesh, for example all corners around node 3 in Fig.2). By taking the maximum of all these corner limiter values, one builds a modified corner limiter that links corners from different cells together thru this maximum.

4 Numerical results

In order to test these modified limiters, we ran the Noh problem ($t = 0.6$) on a full disk in Cartesian geometry with the polar mesh where each quadrangle is split into four triangles (see Fig.8 third panel). This mesh is built onto a quadrangular mesh obtained with 35 points in radial direction and 35 points in angular directions; each of these quadrangles is split into four triangles by adding a point at their center. Therefore the triangular mesh used for these simulations posses 4655 cells and 2346 points.
We ran this problem on a full disk to avoid any boundary effect due to the limiter. The CFL is set to 1/4 (we tried smaller CFL as well with the same results) and the merit factor for the subpressure method (to kill parasital Hourglass mode, see [7] for details) set to 0.0. (We observed that parasital Hourglass modes are not responsible for this behavior.).

This problem with such a mesh leads to relatively bad results with the original limiters, as we already saw in the previous section, for the tensor artificial viscosity. The edge-based viscosity is not able to produce any better results on this problem (see [8]). Therefore we focus on improving the results on this particular problem expecting a general improvement for other problems.

No limiter: Results are plotted in Fig.11. There is no lack of symmetry, and the angular resolution plays a role for the accuracy (which should not be the case with a good limiter see Fig.4).

Original limiter: Results are plotted in Fig.12 as described in this paper. We already know that this limiter is not adapted to this context, but we need a reference result to compare with.

Original edge-based limiter: Results are plotted in Fig.13. This limiter was described in [8] and is edge-based, however Campbell and Shashkov stated that it is not well adapted to the tensor artificial viscosity and developed the corner-based limiter from the previous paragraph. As already noticed some instabilities appear close to the center.

Cell-based limiter: In order to compute the cell-based limiter one can choose to use the original corner-based limiter (see Fig.14 top panels) or the original edge-based limiter (see Fig.14 bottom panels) as building brick. This leads to two different cell-based limiters. However both of them are not able to cure the bad behaviors as can be seen on the results.

Modified Corner-based limiter: The modified corner limiter is used in this case and produces the results in Fig.15; no improvement can be seen.

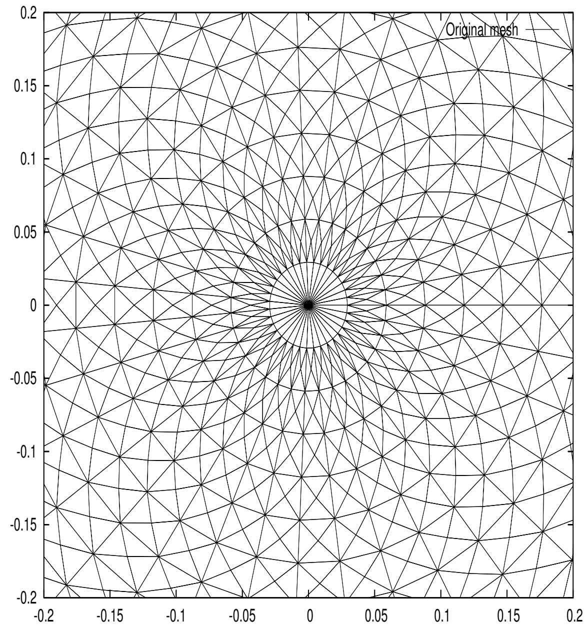

Figure 10: Initial mesh used for the simulation (zoomed on the center) — This mesh is built onto a quadrangular mesh obtained with 35 points in radial direction and 35 points in angular directions; each of these quadrangles is split into four triangles by adding a point at their center. Therefore this triangular mesh used for these simulations possess 4655 cells and 2346 points.

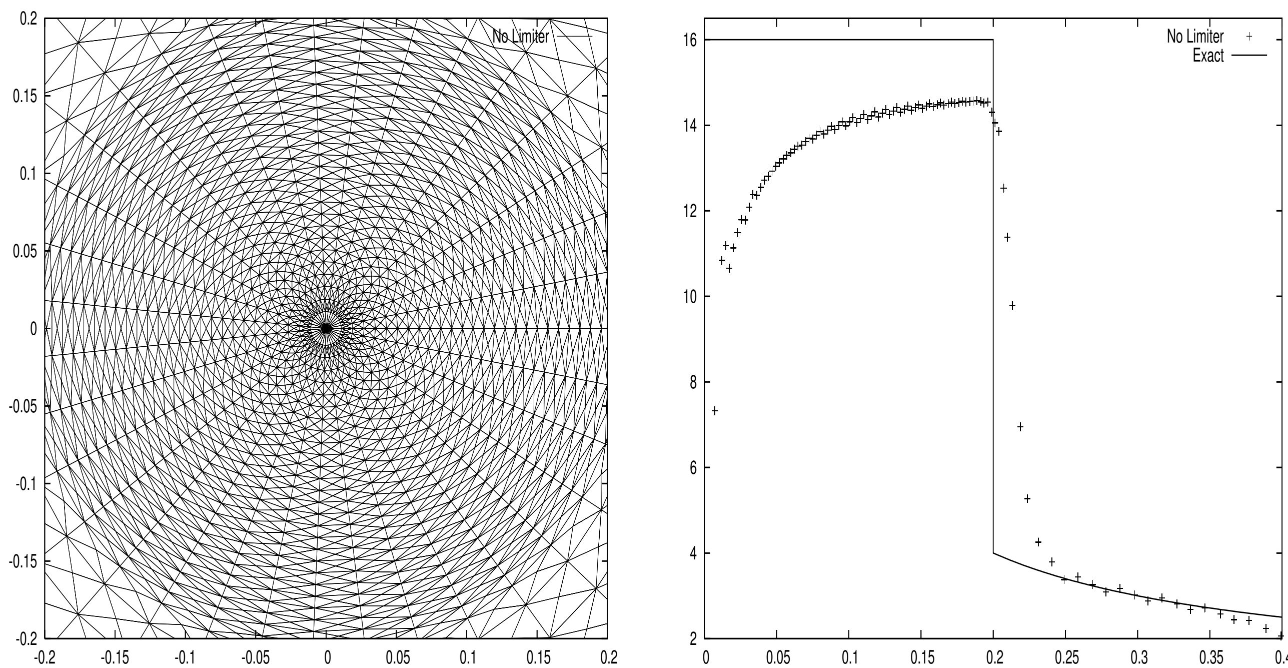

Figure 11: Noh problem at $t = 0.6$ — Left: Final mesh — Right: Cell density as a function of radius *vs* exact solution — No limiter is used for the tensor artificial viscosity; symmetry is preserved

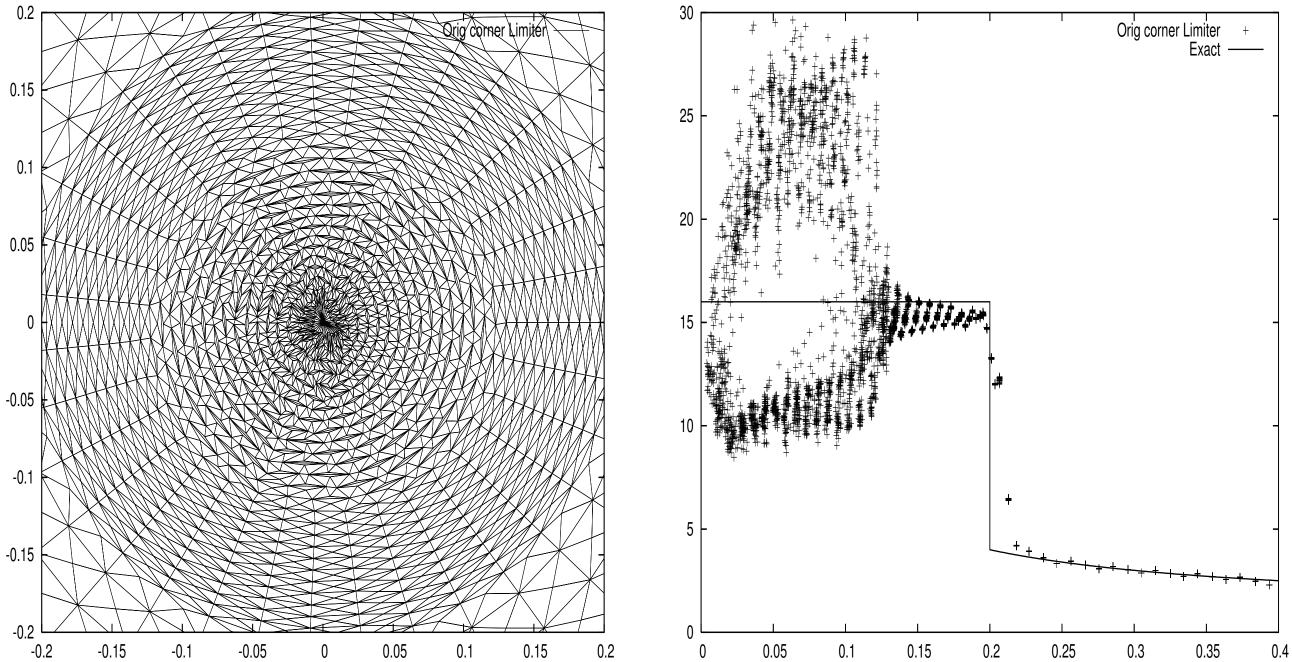

Figure 12: Noh problem at $t = 0.6$ — Left: Final mesh — Right: Cell density as a function of radius *vs* exact solution — The original corner limiter for the tensor artificial viscosity is used, it produces unexpected instabilities.

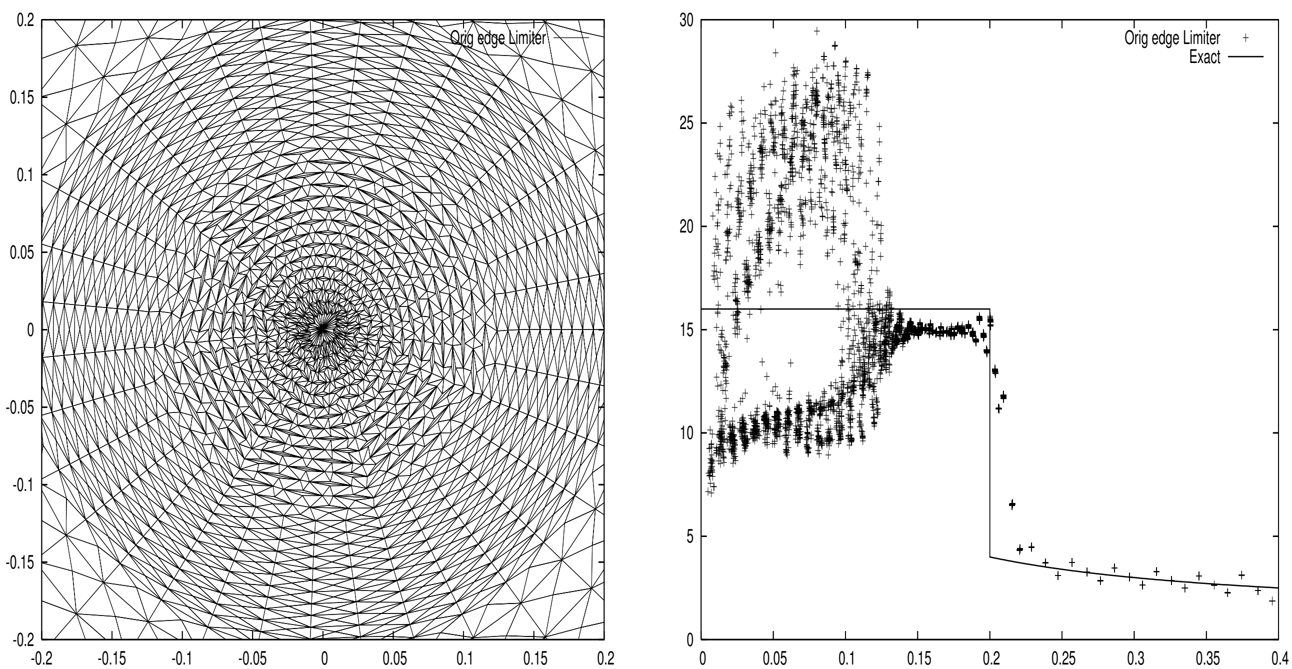

Figure 13: Noh problem at $t = 0.6$ — Left: Final mesh — Right: Cell density as a function of radius *vs* exact solution — The original edge limiter for the tensor artificial viscosity is used, it produces unexpected instabilities.

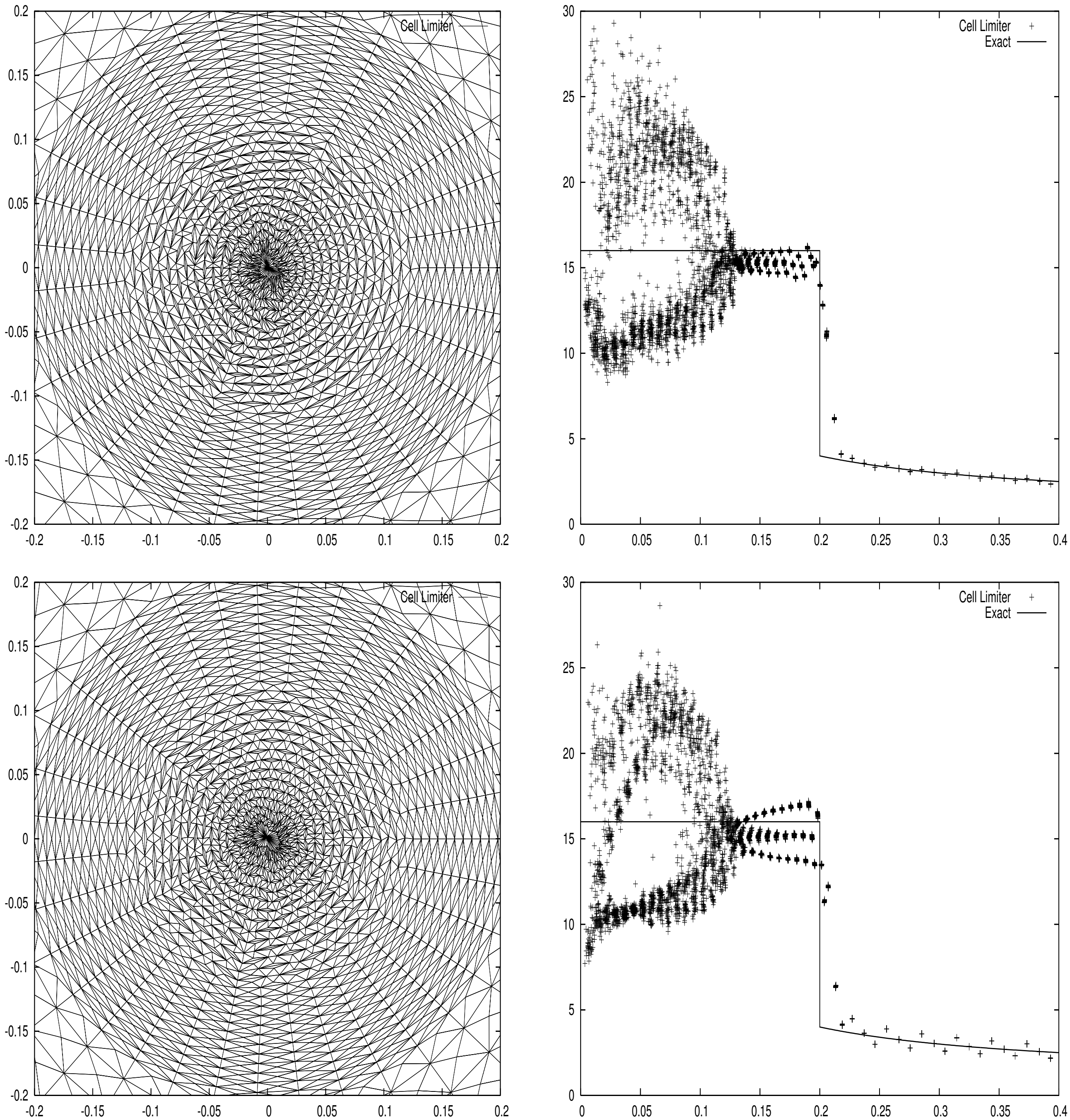

Figure 14: Noh problem at $t = 0.6$ — Left: Final mesh — Right: Cell density as a function of radius *vs* exact solution — **Top:** The cell-based limiter for the tensor artificial viscosity is used (with the original corner limiter as a building brick) — **Bottom:** The cell-based limiter for the tensor artificial viscosity is used (with the original edge limiter as a building brick). These limiter modifications still produce unexpected instabilities.

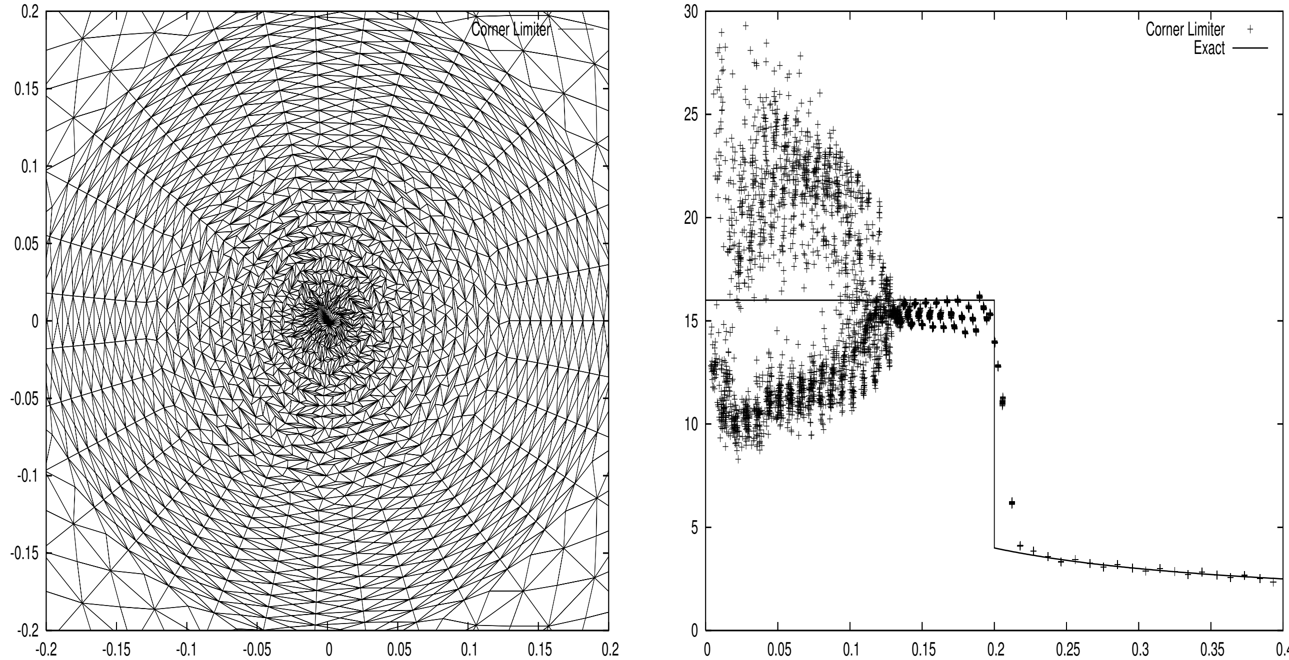

Figure 15: Noh problem at $t = 0.6$ — Left: Final mesh — Right: Cell density as a function of radius *vs* exact solution — The modified corner limiter for the tensor artificial viscosity is used, it produces unexpected instabilities.

Modified Edge-based limiter: The modified edge limiter is used in this case and produces the results in Fig.16. Clearly such a modification does not help in this context.

5 Conclusions

In this report we present the first results obtained as to study and eventually modify the existing limiter in the tensor artificial viscosity as described in [6].

The purpose of a limiter is to turn off the artificial viscosity along phase front where compression occurs only due to convergent symmetry for example. In this case the angular resolution should not play any role as far as the accuracy is concerned: the limiter ensures this statement.

Although such a limiter works perfectly fine with a nicely aligned mesh, it does not anymore when the mesh is unstructured or simply not aligned.
Our goal was to describe very simple reasonable modifications that can be made to such a limiter and prove numerically that such simple modification did not improve the bad behavior one can observe on the Cartesian Noh problem in 2D on a triangular mesh. The triangular mesh is obtained from the polar quadrangular mesh by splitting each quadrangle into four triangles after the introduction of a new point at the center of the quadrangle.

The modifications made to the limiter did not lead to any improvement of the behavior for this problem; it seems that simple modifications of the limiter are not enough to cure the observed bad behavior on unstructured mesh. It seems that with such limiters the antagonist wish of (i) preserving the symmetry using unstructured meshes **and** (ii) preserving the property of angular independence for converging/diverging cylindrical problem, can not be achieved. More profound changes have to be investigated, maybe not only on the form of the limiter itself but on the concept of limiter if non-aligned meshes have to be used.

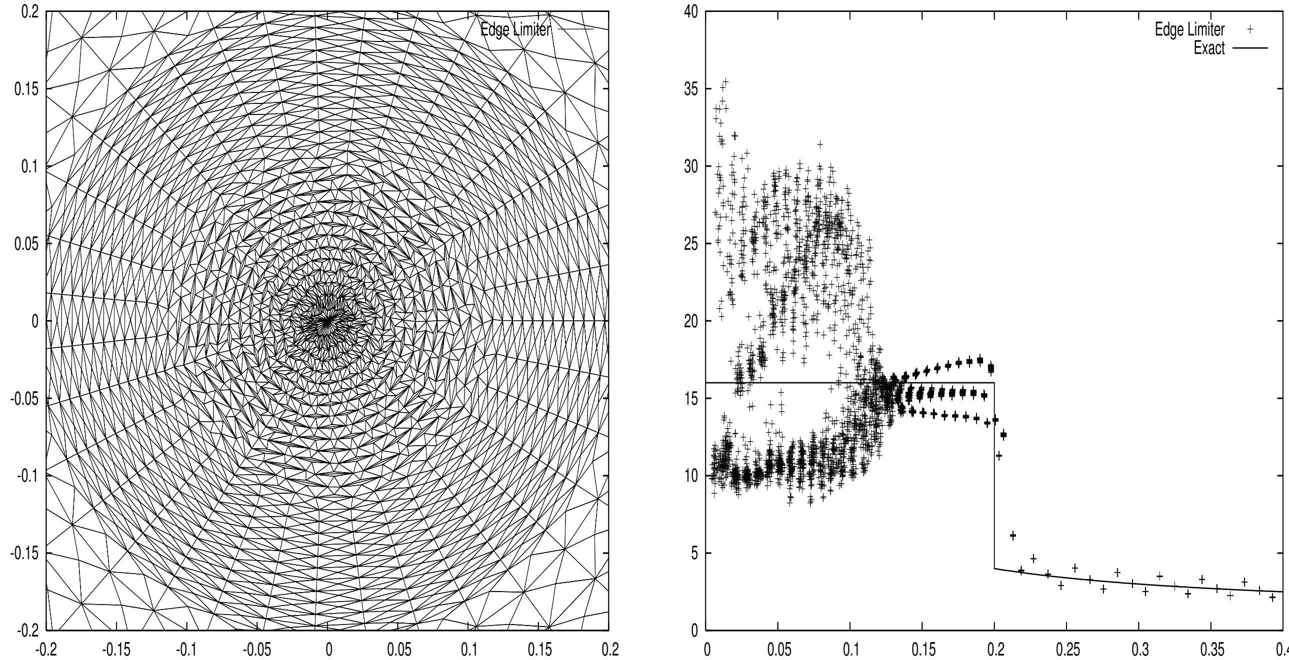

Figure 16: Noh problem at $t = 0.6$ — Left: Final mesh — Right: Cell density as a function of radius *vs* exact solution — The modified edge limiter for the tensor artificial viscosity is used, it produces unexpected instabilities.

Finally the rather negative conclusions are:

- the concept of limiter for tensor artificial viscosity is only well defined for a mesh aligned with the flow and works well in this context;
- the use of a limiter leads to lack of symmetry and inaccuracy in the solution when an unstructured mesh is used; however if no limiter is added to the artificial viscosity such instabilities do not appear, therefore the form of the core of the artificial viscosity has not to be modified;
- simple modifications on the form of the limiter do not seem to improve this behavior (at least the ones we tried, see the numerical examples);
- the concept of limiter for unstructured grid may have to evolve in the context of unstructured grid;
- using a limiter in the tensor artificial viscosity is less important than for the edge-based artificial viscosity. This point has not been proved in this paper but is obvious by comparing the results from [8] and the ones presented in this report; moreover we carried out some numerical experiments confirming this point.

Acknowledgment: We would like to acknowledge the support of the hydro project from the Los Alamos National Laboratory. We thank M.Shashkov and Ed Caramana for fruitful discussions.

References

[1] V. F. Kuropatenko, *in Difference Methods for Solutions of Problems of Mathematical Physics*, N. N. Janenko, ed., Amer. Math. Soc., Providence, 1967, p. 116.

[2] M. L.Wilkins, *Use of artificial viscosity in multidimensional shock wave problems*, Journal of Computational Physics, **36**, 281 (1980).

[3] J. Von Neumann and R.D. Rychtmyer, *A method the calculation of hydrodynamic shocks.*, Journal of Applied Physics, **21**, (1950) pp.232-237

[4] R.Loubère, *First steps into ALE INC(ubator). A 2D ARBITRARY-LAGRANGIAN-EULERIAN CODE ON GENERAL POLYGONAL MESH FOR COMPRESSIBLE FLOWS Version 1.0.0*, LA-UR-04-8840

[5] J. Campbell and M. Shashkov, *A Compatible Lagrangian Hydrodynamics Algorithm for Unstructured Grids*, Selcuk Journal of Applied Mathematics, **4** (2003) pp. 53–70; report version can be found at (http://cnls.lanl.gov/ shashkov),

[6] J. Campbell, M. Shashkov, *A tensor artificial viscosity using a mimetic finite difference algorithm*, Journal of Computational Physics, **172** (2001), pp. 739–765.

[7] E. J. Caramana and M. J. Shashkov, *Elimination of Artificial Grid Distortion and Hourglass-Type Motions by means of Lagrangian Subzonal Masses and Pressures*, Journal of Computational Physics, **142** (1998), p. 521.

[8] E. J. Caramana, M. J. Shashkov and P. P. Whalen, *Formulations of Artificial Viscosity for Multi-Dimensional Shock Wave Computations*, Journal of Computational Physics, **144** (1998), p. 70.

[9] E. J. Caramana, R. Loubère, *"Curl q": A Vorticity Damping Artificial Viscosity for Lagrangian Hydrodynamics Calculations*, Journal of Computational Physics, 2005 in Review.

[10] E. J. Caramana, D. E. Burton, M. J. Shashkov and P. P. Whalen *The Construction of Compatible Hydrodynamics Algorithms Utilizing Conservation of Total Energy*, Journal of Computational Physics, **146** (1998), p. 227.

[11] J.K.Dukowicz and B.Meltz *Vorticity errors in multidimensional Lagrangian codes*, J. Comp. Phys. **99**, 115 (1992).

[12] W. F. Noh, *Errors for calculations of strong shocks using an artificial viscosity and an artificial heat flux*, J. Comp. Phys. **72**, 78 (1987).

[13] R. Loubère, *Investigation of triangular meshes for compressible Lagrangian hydrodynamics*, Los Alamos National Laboratory, LA-UR-05-2937, (2005).